



HAL
open science

Influence of acoustic streaming on thermo-diffusion in a binary mixture under microgravity

Marie-Catherine Charrier-Mojtabi, Alain Fontaine, Abdelkader Mojtabi

► **To cite this version:**

Marie-Catherine Charrier-Mojtabi, Alain Fontaine, Abdelkader Mojtabi. Influence of acoustic streaming on thermo-diffusion in a binary mixture under microgravity. *International Journal of Heat and Mass Transfer*, 2012, 55 (21-22), pp.5992-5999. 10.1016/j.ijheatmasstransfer.2012.06.009 . hal-00921249

HAL Id: hal-00921249

<https://hal.science/hal-00921249>

Submitted on 20 Dec 2013

HAL is a multi-disciplinary open access archive for the deposit and dissemination of scientific research documents, whether they are published or not. The documents may come from teaching and research institutions in France or abroad, or from public or private research centers.

L'archive ouverte pluridisciplinaire **HAL**, est destinée au dépôt et à la diffusion de documents scientifiques de niveau recherche, publiés ou non, émanant des établissements d'enseignement et de recherche français ou étrangers, des laboratoires publics ou privés.



OATAO is an open access repository that collects the work of Toulouse researchers and makes it freely available over the web where possible.

This is an author-deposited version published in : <http://oatao.univ-toulouse.fr/>
Eprints ID : 10555

To link to this article : DOI: 10.1016/j.ijheatmasstransfer.2012.06.009
<http://dx.doi.org/10.1016/j.ijheatmasstransfer.2012.06.009>

To cite this version : Charrier-Mojtabi, Marie-Catherine and Fontaine, alain and Mojtabi, Abdelkader *Influence of acoustic streaming on thermo-diffusion in a binary mixture under microgravity*. (2012) International Journal of Heat and Mass Transfer, vol. 55 (n° 21-22). pp. 5992-5999. ISSN 0017-9310

Any correspondence concerning this service should be sent to the repository administrator: staff-oatao@listes-diff.inp-toulouse.fr

Influence of acoustic streaming on thermo-diffusion in a binary mixture under microgravity

Marie Catherine Charrier-Mojtabi^{a,*}, Alain Fontaine^a, Abdelkader Mojtabi^{b,c}

^aUniversity of Toulouse, University Paul Sabatier, Laboratoire Phase, EA 3028, 118 Route de Narbonne, F-31400 Toulouse, France

^bUniversity of Toulouse; INPT; UPS; IMFT (Institut de Mécanique des Fluides de Toulouse); Allée Camille Soula, F-31400 Toulouse, France

^cCNRS; IMFT, F-31400 Toulouse, France

A B S T R A C T

An analytical and numerical study of the influence of acoustic streaming on species separation of a binary mixture under microgravity is presented. A rectangular cell filled with binary fluid is submitted to an ultrasonic propagating wave along a portion of one of its small walls while the opposite wall is perfectly absorbing. A temperature gradient is applied between the two other walls. The unicellular flow induced by the Eckart streaming may lead to significant species separation. In a first part, the hypothesis of parallel flow is used to determine the analytical solution which describes the unicellular flow and the separation is calculated analytically based on the acoustic streaming parameter, A , the acoustic beam width, ε , and the Schmidt number, Sc . These analytical results are corroborated by direct numerical simulations. In a second part, a linear stability analysis of the unicellular flow is performed. The eigenvalue problem resulting from the temporal stability analysis is solved by the Galerkin method, a spectral Tau–Chebyshev method and by a finite element method. The thresholds for the stationary and oscillatory instability depend on the normalized acoustic beam width.

Keywords:

Acoustic streaming
Thermogravitation
Soret effect
Species separation
Stability

1. Introduction

The propagation of ultrasonic waves in a fluid may induce a stationary flow at large scale: this phenomenon is called “acoustic streaming”, Lighthill [1], Eckart [2].

A review of most of the pertinent information on the acoustic streaming can be found in the following recent papers. Lei et al. [3], performed 3D numerical experiments in order to investigate the convection in an enclosure subjected to a horizontal temperature gradient and a longitudinal sound field. The authors’ contribution concerns Rayleigh streaming created along the walls by a standing wave in a three-dimensional cavity. The contribution of Dridi et al. [4] concerns Eckart streaming in a three-dimensional cavity. The structure of the flow induced by acoustic streaming and its stability were determined numerically. The authors found that the thresholds increased when the acoustic streaming effect was enhanced. Destabilization effects were also observed for a specific parameter range. Dridi et al. [5] also studied Eckart acoustic streaming in their most recent papers. The authors considered an incompressible liquid layer, of thickness H , confined between two infinite horizontal walls. This layer was subjected to a temperature gradient and to a radiation pressure caused by an ultrasound

beam generated by a transducer. The ultrasound beam, which was applied inside the layer, had a normalized width $\varepsilon = H_b/H$ in the z direction and was uniform in the transverse direction x .

The velocity profiles of the basic flows were determined analytically when the beam was centered on the side of the cavity and in the case where the beam was not centered but was positioned at a given location $z = z_b$.

The authors studied the linear stability of Eckart streaming flows in an isothermal or laterally heated mono-constituent fluid layer in the gravity field. The critical value of the acoustic streaming parameter, A_c , leading to a Hopf bifurcation, was determined in the case of an isothermal flow for an infinite horizontal fluid layer. For a centered beam, A_c is minimum for an acoustic beam width $\varepsilon = 0.32$ and increases when either ε decreases or increases.

In the present paper, the coupling between Eckart streaming and Soret effect in a binary fluid, in weightlessness, was investigated. In accordance with the contribution [5], the Rayleigh streaming influence was not introduced in our model. Dridi et al. [5] showed that the streaming flow induced by a traveling wave, in a channel with a typical height of a few centimeters is predominantly generated by Eckart streaming. The Rayleigh streaming contribution is negligible. Unlike the works developed in [4,5] where the acoustic source was centered or not, in the current study, the beam was always placed in contact with the wall $z = H$ to obtain an unicellular flow. This is a necessary condition to obtain

* Corresponding author. Tel.: +33 (0) 5 61 55 82 25; fax: +33 (0) 61 55 81 54.
E-mail address: cmojtabi@cict.fr (M.C. Charrier-Mojtabi).

Nomenclature

A	acoustic streaming parameter $A = \alpha U_{ac}^2 H^3 / \nu^2$	S	species separation
A_d	modified acoustic streaming parameter $A_d = \alpha U_{ac}^2 H^3 / \nu D$	Sc	Schmidt number, $Sc = \nu / D$
a	thermal diffusivity of the mixture	\vec{V}	flow velocity (m s^{-1})
B	aspect ratio of the cell: $B = L/H$	<i>Greek symbols</i>	
C	mass fraction of the considered component of the mixture	α	amplitude attenuation coefficient for ultrasound wave
C_0	initial mass fraction of the considered component of the mixture	β_c	solulal expansion coefficient
D	mass diffusion coefficient ($\text{m}^2 \text{s}^{-1}$)	β_T	thermal expansion coefficient
D_T	thermodiffusion coefficient ($\text{m}^2 \text{s}^{-1} \text{K}^{-1}$)	ε	normalized acoustic beam width $\varepsilon = H_b/H$
Gr	thermal Grashof number, $Gr = g\beta_T \Delta T H^3 / \nu^2$	σ	temporal amplification of perturbation
H	height of the cavity along the z -axis	ρ	density of the fluid mixture (kg m^{-3})
H_b	height of the acoustic beam	ν	kinematic viscosity of mixture ($\text{m}^2 \text{s}^{-1}$)
L	length of the cavity along the x -axis	<i>Subscripts</i>	
m	mass fraction gradient along the x -axis	c	critical

the separation of species as previously obtained in thermogravitational columns. The ultrasonic waves lead to important species separation for particular values of the acoustic streaming parameter, A , the acoustic beam width, ε and the Schmidt number, Sc .

The combination of two phenomena, convection and pure thermodiffusion, is called thermogravitational diffusion. The coupling of these two phenomena leads, in some circumstance, to large species separation. Clusius and Dickel [6] successfully carried out the separation of gas mixtures in a vertical cavity heated from the side, namely a thermogravitational column (TGC). The optimum separation, between the two ends of the cell is obtained for an appropriate choice of the convective velocity and the mass diffusion time. This optimum is obtained for a very small thickness of the vertical cell. In a vertical thermogravitational column the thermal gradient applied on the wall induces simultaneously a pure diffusion phenomenon and a natural convection flow. Furry, Jones and Onsager [7] developed a fundamental theory to interpret the experimental processes of isotope separation. Lorenz and Emery [8] introduced a porous medium in the TGC columns to increase the separation. More recently, many works were carried out with the aim to increase the separation and to study the linear stability of Soret-driven convection in different configurations. Platten et al. [9] used a tilted thermogravitational column. Experiments were performed with water–ethanol mixtures. Bou-Ali et al. [10] were interested in mixtures with negative Soret coefficient in the TGC. Elhajjar et al. [11] developed a linear stability analysis of the unicellular flow which appears when the separation ratio is higher than a certain positive value, in a Rayleigh–Bénard configuration. Zebib and Bou-Ali [12] performed a linear stability analysis of a binary mixture buoyant return flow in a tilted differentially heated infinite layer using asymptotic long-wave analysis and pseudo-spectral Chebyshev numerical solutions. Elhajjar et al. [13] presented a theoretical and numerical study of species separation in an inclined porous cavity.

In the present configuration, in order to obtain an analytical solution of the unicellular flow, a shallow cavity along the x direction is considered ($B = L/H \gg 1$, B being the aspect ratio of the rectangular cavity). A portion of one of its small sides along the z axis is submitted to an ultrasonic propagating wave while the opposite wall is a perfectly absorbing wall. The sides along the x axis are maintained at uniform temperature T_1 and T_2 , respectively. The normalized width ε of the acoustic beam varies between 0 and 1, and the beam is applied from the top of the cell ($z = H$). Acoustic streaming describes a steady flow generated by an ultrasound wave propagating in a fluid. This effect was first observed in

1831 by Faraday [14]. It is well known that it is a non linear phenomenon whose origin is due to Reynolds stress and the dissipation of the acoustic energy flux. Nyborg [15] showed that a constant radiation pressure associated to an ultrasonic traveling wave and generated in a given direction (x direction in our configuration) is associated to a body force oriented along the x axis. Its intensity is given by: $F = \rho \alpha U_{ac}^2 e^{-2\alpha x}$, where α is the amplitude attenuation coefficient for an ultrasound wave, and U_{ac} is the amplitude of the acoustic velocity oscillation. This expression of the force F is valid under the assumptions of plane wave and negligible divergence of the beam. Under the assumption that the attenuation of the wave is sufficiently weak, the body force is considered as a constant $F = \rho \alpha U_{ac}^2$ inside the beam of height H_b , and equal to zero outside the beam. This body force can be introduced in the Navier–Stokes equations [1].

The species separation per unit of length, m , was calculated as a function of the acoustic streaming parameter A , Sc and ε . These analytical results were corroborated by direct 2D numerical simulations. The linear stability analysis of the unicellular flow, performed for an infinite layer, showed that the unicellular flow loses its stability via Hopf bifurcation for all the values of the acoustic beam width, ε , except for $\varepsilon = 0.5$ for which the transition is a stationary one.

2. Mathematical formulation

We consider a rectangular cavity of large aspect ratio $B = L/H$, where H is the height of the cavity along the z -axis and L is the length along the x -axis. The cavity is filled with a binary fluid mixture of density ρ and dynamic viscosity μ . The two walls $x = 0$ and $x = L$ are adiabatic and impermeable. The two other walls $z = 0$ and $z = H$ are kept at uniform temperature T_1 for $z = 0$ and T_2 for $z = H$. The mathematical formulation is presented taking into account the gravity field in order to obtain the general formulation: $\vec{g} = -g\vec{e}_z$ (Fig. 1). The Boussinesq approximation is assumed valid, thus, the thermo-physical properties of the binary fluid are constant, except the density in the buoyancy term which varies linearly with the local temperature T and the mass fraction C of the considered component;

$$\rho = \rho_0 [1 - \beta_T (T - T_{ref}) - \beta_C (C - C_{ref})] \quad (1)$$

where β_T and β_C are respectively the thermal and mass expansion coefficients of the binary fluid.

The dimensionless mathematical formulation of the problem is given by:

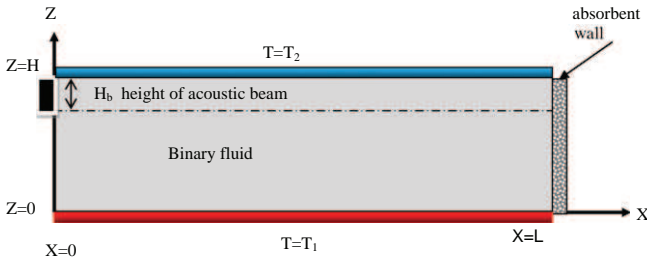


Fig. 1. Geometrical configuration of the cell submitted to an ultrasound beam.

$$\begin{cases} \nabla \cdot \vec{V} = 0 \\ \frac{D\vec{V}}{Dt} = -\nabla P + A \delta \vec{e}_x + Gr(T + \psi C) \vec{e}_z + \nabla^2 \vec{V} \\ \frac{\partial T}{\partial t} + \vec{V} \cdot \nabla T = \frac{1}{Pr} \nabla^2 T \\ \frac{\partial C}{\partial t} + \vec{V} \cdot \nabla C = \frac{1}{Sc} (\nabla^2 C - \nabla^2 T) \end{cases} \quad (2)$$

where the parameter δ , in the system (2), is defined by: $\delta = 1$ for $z \in [1 - \varepsilon, 1]$ and $\delta = 0$ for $z \in [0, 1 - \varepsilon]$.

The reference scales are H for the length, ν/H for the velocity (ν is the kinematic viscosity of the binary fluid), H^2/ν for the time, $\Delta T = T_1 - T_2$ for the temperature, and $\Delta C = -\Delta T C_0 (1 - C_0) (D_T/D)$ for the mass fraction, where D_T and D are, respectively, the thermo-diffusion and mass-diffusion coefficient of the considered component. The problem under consideration depends on six non-dimensional parameters: the thermal Grashof number, $Gr = g\beta_T H^3 \Delta T / \nu^2$, the acoustic streaming parameter $A = \alpha U_{ac}^2 H^3 / \nu^2$, the Schmidt number $Sc = \nu/D$, the separation ratio $\psi = -(\beta_c / \beta_T) (D_T/D) C_0 (1 - C_0)$ where C_0 is the initial mass fraction of the considered component, $\varepsilon = H_b/H$, the normalized acoustic beam width and the aspect ratio of the cell $B = L/H$.

The corresponding dimensionless boundary conditions are:

$$z = 0, 1 : \vec{V} = \vec{0} \quad \frac{\partial T}{\partial z} - \frac{\partial C}{\partial z} = 0; \quad x = 0, x = B : \vec{V} = \vec{0} \quad \frac{\partial T}{\partial x} = \frac{\partial C}{\partial x} = 0 \quad (3)$$

Note: If we choose $\Delta C = -\Delta T (\beta_T / \beta_c)$ rather than $\Delta C = -\Delta T C_0 (1 - C_0) (D_T/D)$ as reference scale for the mass fraction, the separation ratio, ψ , will appear in the right-hand-side term of the species equation and in the boundary conditions but it will not be present in the Navier-Stokes equation.

3. Analytical solution in the case of a shallow cavity: unicellular flow in microgravity ($Gr = 0$)

3.1. Closed-form analytical solution

In the case of a shallow cavity $B \gg 1$, in microgravity (i.e. $Gr = 0$), the parallel flow approximation, used by many previous authors [11], is considered. The solution corresponding to the unicellular flow is given as follows:

$$\vec{U}_0 = U_0(z) \vec{e}_x \quad T_0 = 1 - z, \quad C_0(x, z) = mx + f(z) \quad (4)$$

where m is the mass fraction gradient along the x axis.

The traveling wave is supposed not to interact with the wall at $z = 1$.

With these assumptions and for the steady state, the system of Eq. (2) with the boundary conditions (3) is reduced to a set of the following equations solved using Maple software:

$$\begin{cases} \left(\frac{d^2 U_0}{dz^2} + A\delta \right) \vec{e}_x - \nabla P_0 = 0 \\ \frac{d^2 T_0}{dz^2} = 0 \\ m U_0 Sc = \frac{\partial^2 C_0}{\partial z^2} \end{cases} \quad (5)$$

The two first equations obtained in the system (5) were considered by Dridi et al. [5]. To solve the system (5), the following assumptions are considered:

- Continuity of the velocity, the stress constraint, the mass fraction and temperature at the interface of the acoustic beam for $z = 1 - \varepsilon$.
- The mass flow rate through any cross section perpendicular to the x -axis is equal to zero.
- The mass flow rate of the component of mass fraction C on all the cell is equal to zero.

Thus the expression of the velocity, the mass fraction and the temperature field are given by the following expressions:

$$U_0(z) = -\frac{1}{2} A \varepsilon^2 z (2\varepsilon z - 3z - 2\varepsilon + 2) \quad \text{for } 0 \leq z \leq 1 - \varepsilon$$

$$U_0(z) = -\frac{1}{2} A (\varepsilon - 1)^2 (z - 1) (2\varepsilon z + z - 1) \quad \text{for } 1 - \varepsilon \leq z \leq 1$$

$$C_0(x, z) = mx + f_1(z, A, B, m, Sc, \varepsilon) \quad \text{for } 0 \leq z \leq 1 - \varepsilon$$

$$C_0(x, z) = mx + f_1(z, A, B, m, Sc, \varepsilon) - \frac{1}{24} A Sc m (\varepsilon + z - 1)^4 \quad \text{for } 1 - \varepsilon \leq z \leq 1$$

$$T_0(z) = 1 - z \quad \text{for } 0 \leq z \leq 1 \quad (6)$$

$$\text{where } f_1 = \frac{m Sc A \varepsilon^2 [(15 - 10\varepsilon)z^4 - 20(1 - \varepsilon)z^3 + (2 - 3\varepsilon + \varepsilon^3)]}{120} + z - \frac{1 + mB}{2}.$$

The flow velocity component $U_0(z)$ is thus proportional to the intensity of the acoustic parameter A . The expressions (6) giving the velocity are a particular case of those obtained by Dridi et al. [5] for a non-centered beam. Our case corresponds to a particular condition $z_b + H_b/2 = 1/2$, where z_b is the coordinate of the center of the beam with respect to the centre of the layer and $H_b = \varepsilon$ in the nomenclature of the paper [5]. For a given value of A , the maximum velocity U_{\max} is obtained for:

$$\varepsilon_1 = (-1 + \sqrt{13})/6 \approx 0.434 \quad \text{at } z_1 = (1 + \sqrt{13})/6$$

$$\approx 0.768 \quad \text{and for } \varepsilon_2 = (7 - \sqrt{13})/6 \approx 0.566 \quad \text{at } z_2$$

$$= (5 - \sqrt{13})/6 \approx 0.232 \quad \text{with } U_{\max} = \pm A (-46 + 13\sqrt{13})/54$$

$$\approx \pm 0.0162A.$$

These two sets of values (ε_1, z_1) and (ε_2, z_2) are symmetrical with respect to the point $(\varepsilon = 1/2, z = 1/2)$ and verify the two following relations: $\varepsilon_2 + \varepsilon_1 = 1$ and $z_2 + z_1 = 1$.

In Section 4 an interpretation of this result is provided.

The choice of ε_1 or ε_2 leading to the maximum velocity affects the time required for the species separation, S (§3.2).

The velocity profile is presented, in Fig. 2, for $\varepsilon = 0.2$, $\varepsilon = 0.5$ and $\varepsilon = 0.8$ for $A = 0.45$, value of the acoustic parameter for which the species separation is maximum for $Sc = 700$ (see § 3.2). It can be observed that the velocity profile is symmetrical with respect the point $(z = 1/2, U_0 = 0)$ only for $\varepsilon = 0.5$. Thus, the velocity profiles for $\varepsilon = 0.2$ and 0.8 for $A = 0.45$ are symmetrical to one another with respect to the point $(U_0(z) = 0, z = 0.5)$. Similar profiles, corresponding to beams along the boundaries (width = 0.3), were obtained by Dridi et al. [5].

As ε tends to 0 or 1, the velocity profile generated across the cell by the ultrasonic wave is similar to the one obtained when a constant tangential velocity U_x is applied in $z = 1$ or 0. Indeed, at the boundaries $z = 0$ or 1 the velocity is equal to zero in the presence of acoustic streaming and equal to U_x when a constant tangential velocity is applied to one of the horizontal walls. (Fig. 3). Note that when ε tends to 0 or 1, the velocity profiles at constant A tend towards zero amplitude profiles.

Note: In all the following sections, the Schmidt number is $Sc = 700$ corresponding to a water-ethanol binary fluid where the values of Lewis number and Prandtl number are around 100 and 7 respectively.

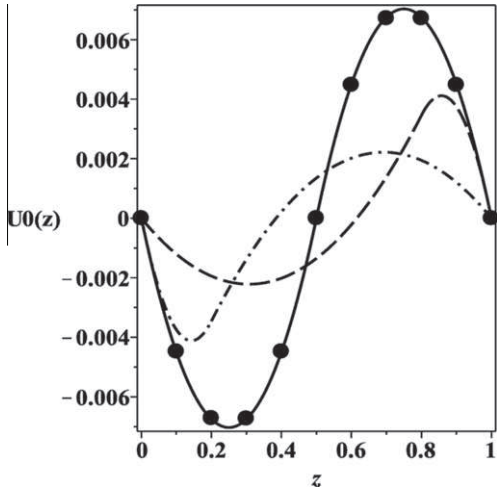


Fig. 2. Velocity profile $U_0(z)$ obtained analytically for $A = 0.45$ and $\varepsilon = 0.2$: dashed line, $\varepsilon = 0.5$; solid line, $\varepsilon = 0.8$; dashed-and-dotted line. Solid circles give the velocity profile obtained in a two dimensional cavity at mid-length for $A = 0.45$ and $\varepsilon = 0.5$ and $B = 10$.

3.2. Study of the species separation, S

The species separation in the binary mixture is studied in this section. The separation S is defined as the difference in mass fraction of the considered species between the two ends of the cell, $x = 0$ and $x = B$, and its expression is $S = mB$, with m defined as:

$$m = -\left(\frac{105}{2}\right) \frac{A Sc \varepsilon^2 (1 - \varepsilon)^2}{A^2 Sc^2 \varepsilon^4 (\varepsilon^2 - \varepsilon - 3)(1 - \varepsilon)^4 - 1260} \quad (7)$$

As indicated in Eq. (7), the separation $S = mB$ is function of A , Sc , ε and B (concentration gradient m does not depend on B). The expressions giving the mass fraction C_0 (Eq. (6)) and the mass fraction gradient m (Eq. (7)) depend on A and on Sc but only via the product $A Sc$ which can be written $A_d = A Sc = \alpha U_{ac}^2 H^3 / \nu D$ as and called modified acoustic streaming parameter. From the Eq. (7), the mass fraction gradient, m , is equal to 0 when $\varepsilon = 0$ or 1 or when the modified acoustic streaming parameter $A_d = 0$. Indeed, for these particular values of A_d and ε , the binary fluid velocity is equal to zero inside the cell.

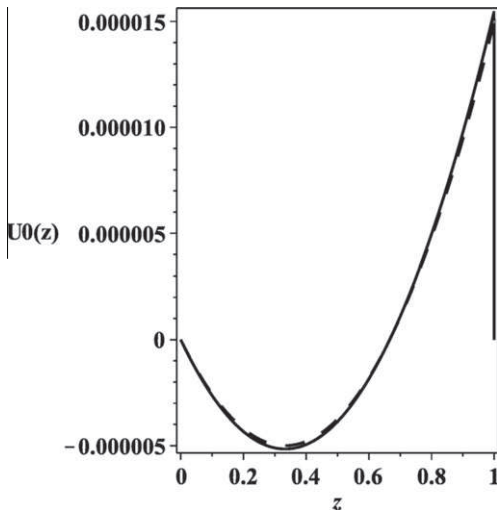


Fig. 3. Comparison between the velocity profile induced by an ultrasonic acoustic wave (solid line: $\varepsilon = 0.001$, $A = 0.643$) and the velocity profile induced in a driven cavity (dashed line: $Pe = 1.5 \times 10^5$; $Pe = \frac{U_a H}{a}$).

The maximum mass-fraction gradient m_{\max} with respect to ε is obtained analytically using Eq. (7) for $\varepsilon = 0.5$ when $A_d \leq \frac{192\sqrt{455}}{13} \cong 315.04$. In this range, there is an increase of m_{\max} with A_d from 0 to $m = \frac{\sqrt{455}}{52} \cong 0.41$. For $A_d > \frac{192\sqrt{455}}{13} \cong 315.04$, m_{\max} is no more obtained for $\varepsilon = 0.5$ but for two values of ε , which are symmetric with respect to $\varepsilon = 0.5$ and which evolve with A_d . In this second range, m_{\max} increases slowly and reaches $m \cong 0.427$ when ε tends to 0 or 1.

These values are close to the one obtained for the thermo-gravitational columns (TGC). For a horizontal porous cell saturated by binary fluid, the optimum value of m is 0.45 [13]. To highlight this result, the curves of the mass fraction gradient, m , versus ε are plotted for four values of A_d (230, 315.04, 1428 and 1428.10^2) in Fig. 4. A symmetry of the curves with respect to $\varepsilon = 0.5$ can be observed in Fig. 4. This result is to be expected as the experiment takes place in microgravity.

In Table 1, we present the different values of the mass fraction gradient obtained analytically for $A_d \in [0, 14285]$ and in Fig. 5 the evolution of the mass fraction gradient versus A_d for $\varepsilon = 0.5$.

4. Numerical simulations

The system of Eq. (2) (with $Gr = 0$) associated to the boundary conditions (3) is solved numerically using a finite element code

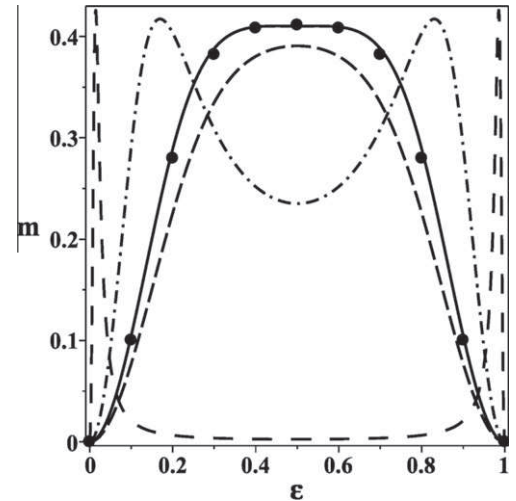


Fig. 4. Mass fraction gradient m versus the acoustic beam width ε , for $A_d = 230$ (dashed line), $A_d = 315.04$ (solid line), $A_d = 1428$ (dashed-and-dotted line) and $A_d = 1428 \times 10^2$ (large space dashed line). Solid circles give the mass fraction gradient m versus ε obtained in a two dimensional cavity for $A_d = 315.04$ and $B = 10$.

Table 1
Analytical values of the mass fraction gradient m versus the acoustic parameter A_d for $\varepsilon = 0.5$.

A_d	m
0	0
600/7	0.2078
1500/7	0.3815
1900/7	0.4057
2100/7	0.4097
2200/7	0.4100
2300/7	0.4098
$4 \times 10^3/7$	0.3469
$5 \times 10^3/7$	0.3029
10^3	0.2351
$10^4/7$	0.1725
$2 \times 10^4/7$	0.0894
$6 \times 10^4/7$	0.0301
$10^5/7$	0.0181

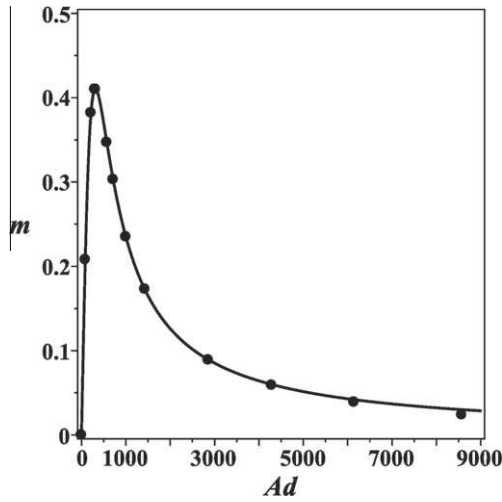


Fig. 5. Analytical curve of the mass fraction gradient m versus the acoustic parameter A_d for $\varepsilon = 0.5$. Solid circles give the mass fraction gradient m versus A_d obtained in a two dimensional cavity for $\varepsilon = 0.5$ and $B = 10$.

(Comsol industrial code) with a rectangular grid, better suited to the rectangular configuration. For the computations, an aspect ratio $B = 10$ is considered. The quadrangle spatial resolution is 120×20 or 150×30 for high values of the modified acoustic streaming parameter A_d .

In order to eliminate the boundary effect, to determine the separation, the curve $C = g(x)$ is plotted at a given value of z ($z = 0.5$ for instance) and the slope of the curve, which is a straight line in the central part of the cell, is calculated.

As mentioned in § 3, in Fig. 4, the numerical results obtained for m versus ε are reported on the curve determined analytically for $A_d = 315.04$. A very good agreement is observed between analytical and numerical results. A similar result is also observed in Figs. 2 and 5.

The mass fraction field, obtained for $A_d = 315.04$ is presented for four values of ε : $\varepsilon = 0.1, 0.5, 0.8, 0.9$, and $\varepsilon = 1$, in Fig. 6. The black lines represent the iso-concentrations. As expected the mass fraction gradient values m , obtained for $\varepsilon = 0.1$ and 0.9 are equal. Indeed for a given value of the acoustic streaming parameter A , the unicellular flow induced by an acoustic beam of thickness ε is opposite to the flow generated by an acoustic beam of thickness

$(1-\varepsilon)$ positioned on the top of the opposite side. This unicellular flow is also identical to the flow generated by an acoustic beam of thickness $(1-\varepsilon)$ positioned on the bottom of the opposite side of the cell. Therefore, this study can be limited to ε varying from 0 to 0.5 or ε varying from 0.5 to 1.

The evolution of the mass fraction field is presented, in Fig. 7, for $A_d = \frac{100}{\varepsilon}$ (0, 6, 22, 50, 100, 200, 600, 1000) and for $\varepsilon = 0.5$.

For very small values of A_d , the concentration field stratification is horizontal and for values of A_d exceeding $A_{dopt} = 315.04$ there is a significant deformation of the mass fraction field leading to a small separation.

5. Linear stability analysis of the unicellular flow

In order to analyze the stability of this unicellular flow described in § 3, the perturbations of velocity $\vec{v} = (u, v, w)$, of temperature θ , of mass fraction c and pressure p are first introduced. The perturbations (\vec{v}, θ, c, p) are assumed to be of small amplitude, then, after simplification the following linearized equations are obtained:

$$\begin{cases} \frac{\partial}{\partial t} \nabla^2 w + U_0 \frac{\partial}{\partial x} \nabla^2 w - \frac{\partial w}{\partial x} \frac{\partial^2}{\partial z^2} (U_0) - \nabla^4 w - Gr \frac{\partial^2}{\partial x^2} (\theta + \psi c) = 0 \\ \frac{\partial \theta}{\partial t} + U_0 \frac{\partial \theta}{\partial x} - \frac{1}{Pr} \nabla^2 \theta + w = 0 \\ \frac{\partial^2 c}{\partial t \partial x} + U_0 \frac{\partial^2 c}{\partial x^2} - m \frac{\partial w}{\partial z} + \frac{\partial}{\partial x} (w \frac{\partial c}{\partial z}) - \frac{1}{Sc} \frac{\partial}{\partial x} (\nabla^2 (c - \theta)) = 0 \end{cases} \quad (8)$$

The associated boundary conditions are:

$$w = \theta = 0, \quad \text{and} \quad \frac{\partial \theta}{\partial z} = \frac{\partial c}{\partial z} \quad \text{for } z = 0 \text{ and } z = 1 \quad \forall x, y, t \quad (9)$$

In microgravity the Grashof number, Gr , is equal to zero. The second and the third equations of the system (8) are decoupled from the first one which involves only the perturbation velocity component w .

The stability of the basic flow is then investigated, using only the first equation of system (8), by a temporal linear analysis. The perturbation quantities are chosen as follows:

$$w = \tilde{w}(z) \exp(ikx + Ihy + \sigma t) \quad (10)$$

where k and h are the wavenumbers respectively in the x and y directions, $I^2 = -1$, and $\sigma = \omega_r + I\omega$ is a complex eigenvalue. The real part of σ , ω_r , represents an amplification rate and its imaginary part, ω , the Hopf pulsation.

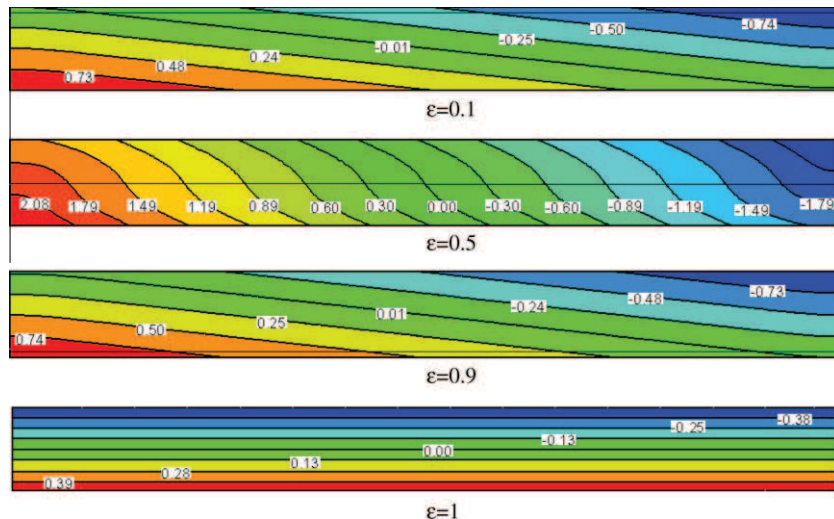


Fig. 6. Mass fraction fields and iso-concentrations for different values of ε and A_{dopt} .

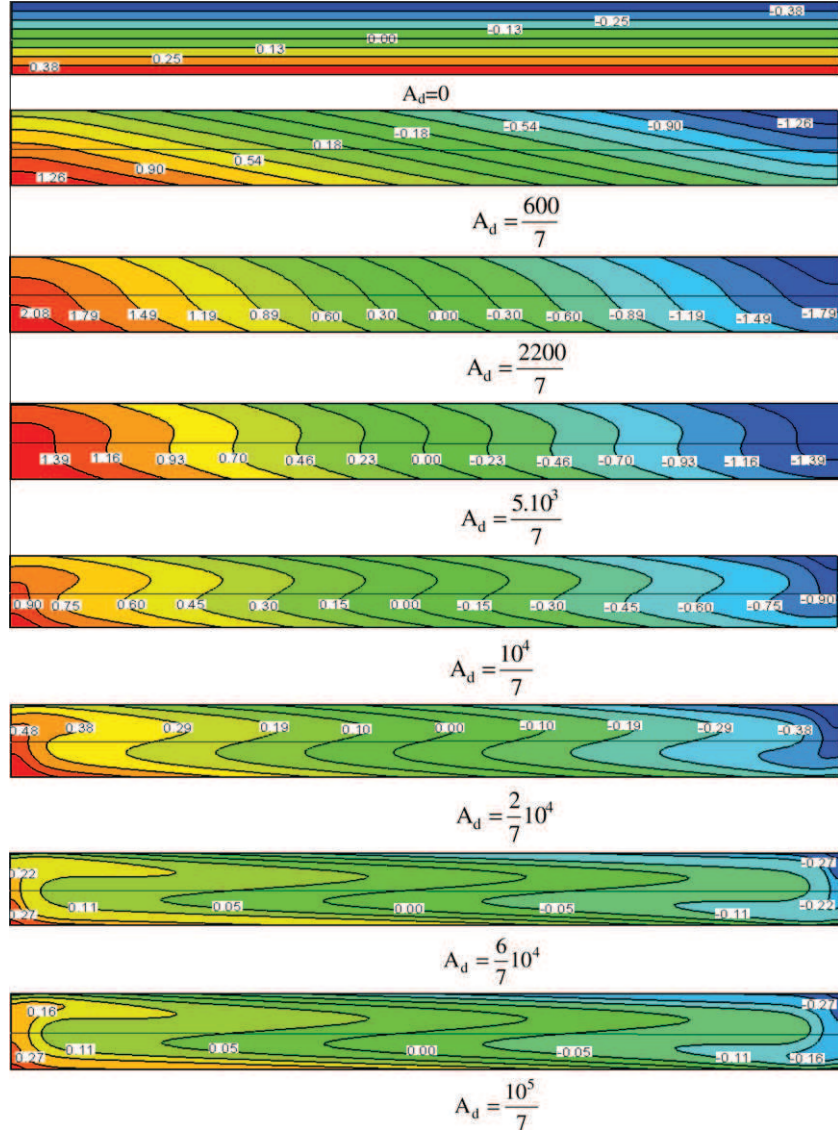


Fig. 7. Mass fraction fields and iso-concentrations for different values of A_d ; $\varepsilon = 0.5$.

Of interest are the instabilities leading to convective rolls with axis perpendicular to the direction of the base flow due only to ultrasonic waves in microgravity, therefore, the wavenumber h is equal to zero. For $Gr = 0$, the first equation of system (8), after substituting w by its expression given by Eq. (10), leads to a fourth order equation depending only on the velocity component $\tilde{w}(z)$:

$$\xi^2(\tilde{w}) - (\sigma + IkU_0)\xi(\tilde{w}) + Ik\tilde{w}\frac{d^2}{dz^2}(U_0) = 0 \quad (11)$$

where the derivative operators $\xi = \frac{d^2}{dz^2} - k^2$ and $\xi^2 = \frac{d^4}{dz^4} - 2k^2\frac{d^2}{dz^2} + k^4$.

The same stability problem was treated by Dridi et al. [5] in the case of a non-centered ultra sound beam. However, in the current work, the focus is different as only specific beams along the boundaries are considered. The critical values of the acoustic parameter, A_c , are first determined using the Galerkin method for stationary and Hopf bifurcation: the disturbance \tilde{w} is developed as a polynomial function which verifies all the boundary conditions and the different polynomials obtained when i varies from 1 to N form a complete basis of the studied problem:

$$\tilde{w}(z) = \sum_{i=1}^N a_i(z-1)^{i+1}z^2 \quad (12)$$

The convergence for the resolution using the Galerkin method is obtained for $N \geq 12$.

Two other methods have been used to solve the eigenvalue problem resulting from the temporal stability analysis for the determination of the critical parameters corresponding to either stationary or Hopf bifurcation: a spectral Tau-Chebyshev method with more than 200 collocation points and a finite element method with quadrangle spatial resolution 150×30 . The results obtained by these three methods are in good agreement for both stationary and Hopf bifurcation.

The neutral stability curves describing the evolution of the critical acoustic streaming parameter A_c , Hopf pulsation ω_c and wave length k_c as a function of ε are presented respectively in Figs. 8(a)–8(c). It can be observed that the bifurcation is a stationary one ($\omega = 0$) only for $\varepsilon = 0.5$.

The neutral curve which corresponds to the onset of oscillatory instabilities presents a minimum value for $\varepsilon = 0.5$, associated to a stationary bifurcation characterized by the critical parameters: $A_c = 3019$ and $k_c = 3.33$. The critical value A_c increases and k_c decreases for smaller and higher values of ε around $\varepsilon = 0.5$ while the absolute value of the critical angular frequency increases. The increase of A_c for large or small values of ε , symmetrical with

respect to $\varepsilon = 0.5$, is particularly important indicating that the flows induced by large or small beam widths are particularly stable.

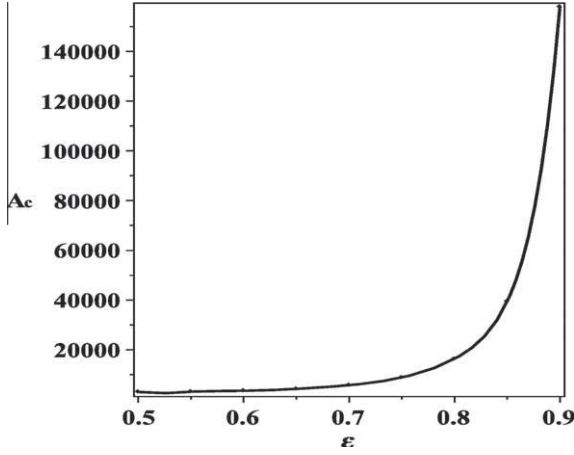


Fig. 8a. Critical values of the acoustic parameter A_c versus ε .

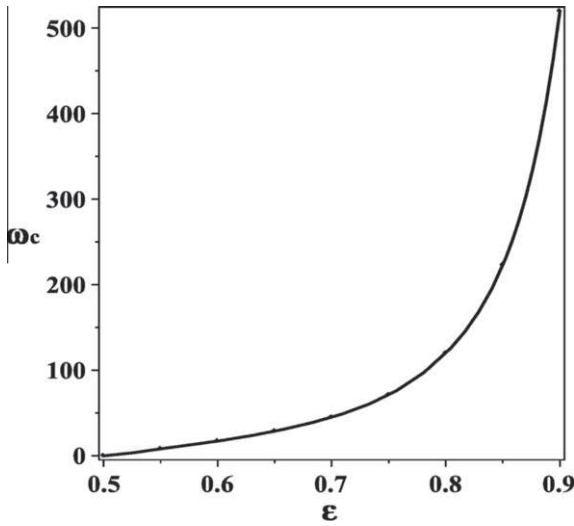


Fig. 8b. Critical values of the pulsation ω_c versus ε .

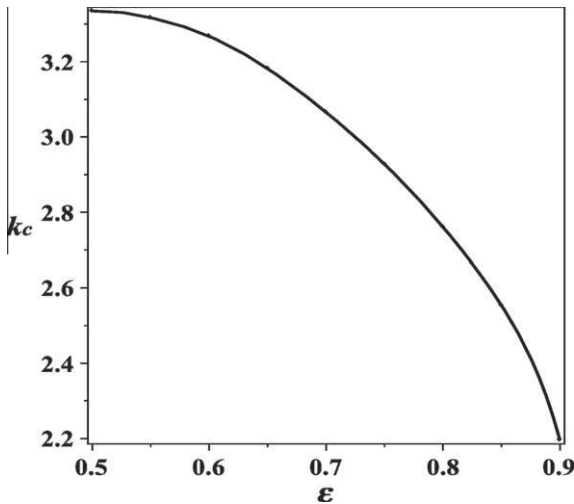


Fig. 8c. Critical values of the wave length k_c versus ε .

Table 2

Values of the critical parameters for different orders of spectral approximation for $\varepsilon = 0.3$ and 0.5 .

Spectral approximation orders	$A_c(\varepsilon = 0.3)$	$k_c(\varepsilon = 0.3)$	ω_c ($\varepsilon = 0.3$)	$A_c(\varepsilon = 0.5)$	$k_c(\varepsilon = 0.5)$
5	5565	3.12	-38.77	3136	3.25
6	5689	3.11	-44.60	3025	3.31
7	5711	3.08	-43.80	3068	3.29
8	5739	3.09	-44.66	3028	3.33
9	5736	3.06	-44.95	3033	3.32
10	5726	3.07	-44.95	3021	3.33
11	5734	3.07	-45.16	3022	3.33
12	5738	3.06	-45.14	3019	3.33
13	5737	3.06	-45.16	3019	3.33
15	5736	3.06	-45.05	3019	3.33
20	5739	3.05	-45.08		
Dridi et al. [5] for $\varepsilon = 0.3$	5700	3.1	-45		

Some particular beams along the boundaries were considered by Dridi et al. [5], namely those corresponding to $z_b = \pm 0.35$ with $\varepsilon = 0.3$. The corresponding results can be found in their Fig. 6, and it can be seen that such beams with $\varepsilon = 0.3$ correspond to instabilities with negative values of the angular frequency ω . We show that for $\varepsilon = 0.3$ and $\varepsilon = 0.7$ $\omega_d(\varepsilon) = -\omega_d(1 - \varepsilon)$ whereas $A_c(\varepsilon) = A_c(1 - \varepsilon)$ and $k_c(\varepsilon) = k_c(1 - \varepsilon)$. The critical values obtained for $\varepsilon = 0.5$ and 0.3 for different orders of spectral approximation are also presented in Table 2. The values obtained for A_c , ω_c and k_c are in good agreement with those extrapolated from Fig. 6 presented by Dridi et al. [5], for $\varepsilon = 0.3$ and $z_b = \pm 0.35$.

6. Conclusion

In this paper, the influence of the acoustic streaming on species separation in a rectangular cavity, filled with a binary fluid in weightlessness, was presented. A new experimental configuration was considered in order to obtain species separation in a binary mixture. To the authors' knowledge, no work has yet been presented on this topic.

In a first part an analytical solution of the unicellular flow induced by the ultrasound traveling wave was determined using the assumption of parallel flow observed for $B \gg 1$. The velocity profiles were plotted for $\varepsilon = 0.5$ and 0.2 . As expected the velocity profile is symmetrical with respect to $z = 0.5$ only for $\varepsilon = 0.5$. Furthermore the velocity profiles $U_0(z)$ obtained for $\varepsilon = 0.2$ and 0.8 are symmetrical to one another with respect to the point ($U_0(z) = 0, z = 0.5$).

Thus, the mass-fraction gradient m was calculated as function of the acoustic streaming parameter, A , the acoustic beam width, ε , the Schmidt number and its variation was presented as a function of the modified acoustic streaming parameter A_d and ε . The maximum separation was obtained for $\varepsilon = 0.5$ and for $A_{d,opt} = \frac{192\sqrt{455}}{13} \approx 315.04$.

The analytical results were corroborated by direct numerical simulations using a finite element code (Comsol). The mass fraction gradients versus ε were plotted for different values of A_d . The symmetry of the curves $m = f(\varepsilon)$ with respect to $\varepsilon = 0.5$ is thus illustrated. The mass fraction fields were also plotted for different values of ε for $A_{d,opt}$ and for different values of A_d for $\varepsilon = 0.5$. The evolution of the iso-concentrations when A_d increases was also presented.

In a second part a linear stability analysis of the unicellular flow was performed using the Galerkin method, a spectral Tau-Chebyshev method and a finite element method. The results obtained by these three methods were in good agreement. This

study showed that the unicellular flow loses its stability via a Hopf bifurcation for all values of ε , except for $\varepsilon = 0.5$, for which the transition is a stationary one. The values of the critical acoustic parameter A_c obtained for different values of ε are much larger than the optimum value A_{opt} leading to the maximum of separation.

Acknowledgment

We wish to acknowledge the valuable comments made by the anonymous referee and specially his helpful suggestion concerning the reference scales used to obtain the present nondimensional formulation.

References

- [1] J. Lighthill, Acoustic streaming, *J. Sound Vibration* 61 (1978) 391–418.
- [2] C. Eckart, Vortices and streams caused by sound waves, *Phys. Rev.* 73 (1948) 68–76.
- [3] H. Lei, D. Henry, H. Ben Hadid, Numerical study of the influence of a longitudinal sound field on natural convection in a cavity, *Int. J. Heat Mass Transfer* 49 (2006) 3601–3616.
- [4] W. Dridi, D. Henry, H. Ben Hadid, Influence of acoustic streaming on the stability of a laterally heated three-dimensional cavity, *Phys. Rev. E* 77 (2008) 046311.
- [5] W. Dridi, D. Henry, H. Ben Hadid, Stability of buoyant convection in a layer submitted to acoustic streaming, *Phys. Rev. E* 81 (2010) 056309.
- [6] K. Clusius, G. Dickel, Neues Verfahren zur Gasenmischung und Isotroprennung, *Naturwisse* 6 (1938) 546.
- [7] W.H. Furry, R.C. Jones, L. Onsager, On the theory of isotope separation by thermal diffusion, *Phys. Rev.* 55 (1939) 1083–1095.
- [8] M. Lorenz, A.H. Emery, The packed thermal diffusion column, *Chem. Eng. Sci.* 11 (1) (1959) 16–23.
- [9] J.K. Platten, M.M. Bou-Ali, J.F. Dutrieux, Enhanced molecular separation in inclined thermogravitational columns, *J. Phys. Chem. B* 107 (42) (2003) 11763–11767.
- [10] M.M. Bou-Ali, O. Ecenarro, J.A. Madariaga, C.M. Santamaria, J.J. Valencia, Measurement of negative Soret coefficients in a vertical fluid layer with an adverse density gradient, *Phys. Rev. E* 62 (2000) 1420.
- [11] B. Elhajjar, M.C. Charrier-Mojtabi, A. Mojtabi, Separation of a binary fluid mixture in a porous horizontal cavity, *Phys. Rev. E* 77 (026310) (2008) 1–6.
- [12] A. Zebib, M.M. Bou-Ali, Inclined layer Soret Instabilities, *Phys. Rev. E* 79 (2009) 056305.
- [13] B. Elhajjar, A. Mojtabi, P. Costesèque, M.C. Charrier-Mojtabi, Separation in an inclined porous thermogravitational cell, *Int. J. Heat Mass Transfer* 53 (2010) 4844.
- [14] M. Faraday, On the forms and states assumed by fluids in contact with vibrating elastic surfaces, *Philos. Trans. R. Soc. London* 121 (1831) 319–340.
- [15] W.L. Nyborg, in: M.F. Hamilton, D.T. Blackstock (Eds.), *Nonlinear Acoustics*, Academic Press, San Diego, 1998, p. 207.